

51 P.

R-COMP-RS-64-1

SIMULATION BRANCH

N64-22445
Code 1 Cat. 30
+MX51695

DYNAMICS OF A ROTATING
SPACE STATION

By

Dr. Walter P. Krause

OTS PRICE

XEROX

MICROFILM

\$

\$

LIBRARY COPY

MAR 20 1964

LANGLEY RESEARCH CENTER
LIBRARY, NASA
LANGLEY STATION
HAMPTON, VIRGINIA

RESEARCH & DEVELOPMENT APPLICATIONS DIVISION
COMPUTATION LABORATORY

MARSHALL

SPACE
FLIGHT
CENTER

NATIONAL AERONAUTICS AND SPACE ADMINISTRATION

SIMULATION BRANCH

R-COMP-RS-64-1

DYNAMICS OF A ROTATING
SPACE STATION

By

Dr. Walter P. Krause

ABSTRACT

NGC. 22445
22445
Equations describing the reaction of a space vehicle to rotating machinery and to mass motion inside the vehicle are formulated. These equations include a component that has been neglected in most earlier studies, i. e., the angular impulse introduced by the moving mass.

The dynamics of a cylindrical space station rotating around its major axis once every 10 seconds are evaluated numerically. The long cylinder provides the large distance between the axis of rotation and the crew compartment needed to generate comfortable artificial gravity. But the rotating cylinder is known to have little dynamic stability around its longitudinal axis. Nevertheless, the stability characteristics of this configuration are found to be acceptable provided there is as little as 0.2% asymmetry between the major and intermediate moments of inertia.

Detailed investigations were performed on an analog computer. These show the effect of path and timing on the magnitude of the disturbance caused by a mass relocation.

Also analyzed in some detail are ways to minimize roll, either by corrective motion of the astronauts or by a simple control system that uses the gyroscopic torque generated by rotating the body-fixed axis of a flywheel.

author

author

SIMULATION BRANCH

R-COMP-RS-64-1

DYNAMICS OF A ROTATING
SPACE STATION

By

Dr. Walter P. Krause

FEBRUARY 1964

RESEARCH & DEVELOPMENT APPLICATIONS DIVISION
COMPUTATION LABORATORY
GEORGE C. MARSHALL SPACE FLIGHT CENTER

TABLE OF CONTENTS

	Page
LIST OF ILLUSTRATIONS	iii
DEFINITION OF SYMBOLS	iv
SECTION I. INTRODUCTION	1
SECTION II. ANALYSIS	2
A. THE UNDISTURBED SYSTEM	2
B. EFFECT OF MASS MOTION WITHIN THE SYSTEM	10
SECTION III. NUMERICAL EVALUATION	22
A. THE ANALOG COMPUTER PROGRAM	22
B. EFFECT OF ASTRONAUTS' MOTION	26
C. AUTOMATIC CONTROL OF STATION'S ROLL MOTION	30
SECTION IV. EFFECT OF EXTERNAL TORQUES	37
SECTION V. CONCLUSIONS	38
APPENDIX ORIENTATION OF THE PRINCIPAL AXES OF THE SPACE STATION RELATIVE TO THE BODY-FIXED AXES	39
REFERENCES	43
APPROVAL	44
DISTRIBUTION	45

LIST OF ILLUSTRATIONS

Figure	Title	Page
1.	Euler Angles, Transformation from Reference to Body-Fixed Coordinate System	3
2.	Model of Rotating Space Station	13
3.	Response of Station (Given Rotational Symmetry Around Length Axis) to Mass Motion from $x = 15 \text{ m}$, $z = 0$ to $x = 15 \text{ m}$, $z = 1.8 \text{ m}$: (a) ϕ Response, (b) θ Response	15, 16
4.	Analog Computer Program	20B
5.	Response of Station to Motion in Unison of Three Astronauts from $\{12 \text{ m}, 0, 0\}$ to $\{18 \text{ m}, 0, 1.8 \text{ m}\}$ Along Three Different Paths	23
6.	Response of Station to Motion in Unison of Three Astronauts (a-c) in yz Plane, (c, d) in xy Plane, (e-g) Parallel to but Not Along x Axis, (h, i) in Circle in yz Plane	25
7.	Effect of One Astronaut Moving in x Direction Synchronously with Roll: (a) Rotation of Principal Axes by Transfer from $\{18 \text{ m}, 0, 0\}$ to $\{18 \text{ m}, 1.27 \text{ m}, 1.27 \text{ m}\}$, (b) Roll Unaffected by Motion in xy Plane, (c) Damping of Roll (Positive z), (d) Augmentation of Roll (Negative z), (e, f) Roll Unaffected by Motion in Phase with $\dot{\phi}$	27
8.	Correction of Initial Roll Disturbance by Controlled Motion of One Astronaut in yz Plane	29
9.	Correction of Initial Roll Disturbance by Flywheel Control System ($h_c = \text{Angular Impulse of Flywheel}$)..	32
10.	Stabilization by a Gyro	35

DEFINITION OF SYMBOLS

SYMBOL	DEFINITION
X, Y, Z	Space-fixed reference axes
ϕ, θ, ψ	Euler angles
x, y, z	Body-fixed axes
\bar{H}	Angular impulse
$\bar{\Omega}$	Angular velocity
\tilde{I}	Inertia tensor
I	Moment of inertia
p, q, r	Components of angular velocity in body-fixed coordinate system
D	Determinant
ξ, η, ζ	Principal axes
φ, ϑ, ψ	Euler angles between principal axes and reference axes
T	Period
m	Movable mass within space
$\bar{\rho}$	Radius vector of movable mass
\bar{R}	Radius vector of center of gravity in body-fixed coordinate system
M	Total mass of space station
\bar{r}_i	Position vector of mass point in space-fixed coordinate system

DEFINITION OF SYMBOLS (Continued)

SYMBOL	DEFINITION
v	Velocity
h	Angular impulse of rotating machinery
P	Power
L	Torque
E	Energy
α, β, γ	Euler angles between principal axes and reference axes
Subscripts	
c	Of command
F	Of flywheel

A dot over a symbol denotes the first derivative with respect to time.

Two dots over a symbol denote the second derivative with respect to time.

A bar over a symbol denotes a vector.

A tilde (\sim) over a symbol denotes a matrix.

ACKNOWLEDGMENTS

Thanks are due to Mr. Joe T. Howell and Mr. Paul F. Bohn for their work on the analog simulation and to Mr. Addison L. McGarrity, who programmed the digital simulation.

DYNAMICS OF A ROTATING SPACE STATION

By
Dr. Walter P. Krause

FEBRUARY 1964

SECTION I. INTRODUCTION

The environment necessary for the life support of astronauts during extended space flights will probably have to include artificial gravity. During periods of coasting, this will be generated by continuous rotation of the space station around an axis that is sufficiently remote from the crew compartment to exclude extreme variations in the centrifugal forces within the compartment.

Our investigation will be limited to a station of cylindrical shape, since this is the geometry most likely to be used for early flights of long duration. As a further qualification, since the rotating cylinder is highly stable around its two axes of large moment of inertia, only the requirements for stability around the third axis, i. e., the longitudinal axis, will be examined.

SECTION II. ANALYSIS

A. THE UNDISTURBED SYSTEM

In the absence of external torques, the angular impulse of the system remains constant. Let us assume that the angular impulse is aligned with the Z axis of the space-fixed reference coordinate system X, Y, Z (Figure 1). Using the transformation matrix from the reference coordinate system to the body-fixed coordinate system expressed in Euler angles ϕ , θ , ψ , we get the components of the angular impulse in the body-fixed coordinate system x, y, z (Figure 1):

$$\begin{bmatrix} H_x \\ H_y \\ H_z \end{bmatrix} = \begin{bmatrix} \cos\psi \cos\theta & \sin\psi \cos\theta & -\sin\theta \\ \cos\psi \sin\theta \sin\phi - \sin\psi \cos\phi & \sin\psi \sin\theta \sin\phi + \cos\psi \cos\phi & \cos\theta \sin\phi \\ \cos\psi \sin\theta \cos\phi + \sin\psi \sin\phi & \sin\psi \sin\theta \cos\phi - \cos\psi \sin\phi & \cos\theta \cos\phi \end{bmatrix} \begin{bmatrix} 0 \\ 0 \\ H \end{bmatrix} \quad (1)^*$$

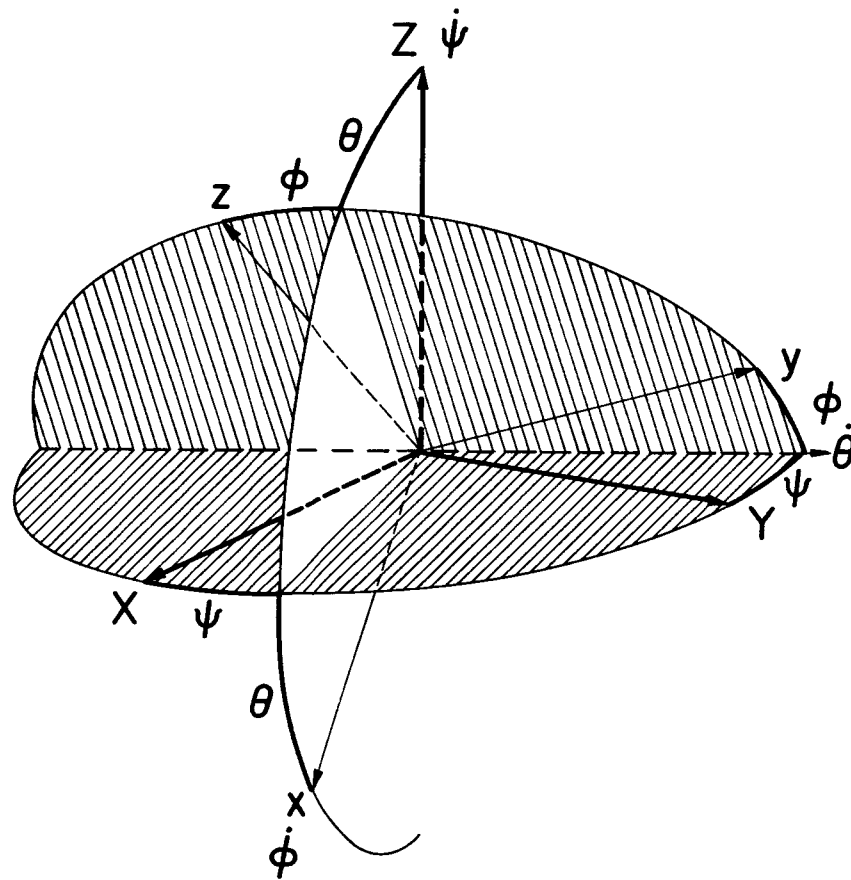
or

$$\begin{aligned} H_x &= -H \sin\theta \\ H_y &= H \cos\theta \sin\phi \\ H_z &= H \cos\theta \cos\phi \end{aligned} \quad (2)$$

The angular impulse is related to the angular velocity by the vector equation

$$\bar{H} = \tilde{I} \cdot \bar{\Omega} \quad (3)$$

* Cf. Fifer, Stanley, Analogue Computation, Vol. IV, New York, McGraw-Hill (1961), pg. 1091



ψ, θ, ϕ AS SHOWN ARE POSITIVE ANGLES.

Figure 1. Euler Angles, Transformation from Reference to Body-Fixed Coordinate System

The inertia tensor \tilde{I} is given by a matrix

$$\tilde{I} = \begin{bmatrix} I_x & -I_{xy} & -I_{xz} \\ -I_{xy} & I_y & -I_{yz} \\ -I_{xz} & -I_{yz} & I_z \end{bmatrix} \quad (4)$$

If there is no mass motion inside the space station, the components of the tensor are constant in the body-fixed coordinate system. Calling the components of the angular velocity in the body-fixed coordinate system p , q , r and using equations (2), the vector equation (3) can be written in components

$$\begin{aligned} H_x &= I_x p - I_{xy} q - I_{xz} r = -H \sin \theta \\ H_y &= -I_{xy} p + I_y q - I_{yz} r = H \cos \theta \sin \phi \\ H_z &= -I_{xz} p - I_{yz} q + I_z r = H \cos \theta \cos \phi \end{aligned} \quad (5)$$

Using determinants, equations (5) are solved for p , q , and r

$$p = \frac{D_1}{D}; \quad q = \frac{D_2}{D}; \quad r = \frac{D_3}{D}; \quad (6)$$

where

$$D = \begin{vmatrix} I_x & -I_{xy} & -I_{xz} \\ -I_{xy} & I_y & -I_{yz} \\ -I_{xz} & -I_{yz} & I_z \end{vmatrix}$$

$$D_1 = \begin{vmatrix} -H \sin \theta & ; & -I_{xy} & ; & -I_{xz} \\ H \cos \theta \sin \phi & ; & I_y & ; & -I_{yz} \\ H \cos \theta \cos \phi & ; & -I_{yz} & ; & I_z \end{vmatrix}$$

$$D_2 = \begin{vmatrix} I_x & ; & -H \sin \theta & ; & -I_{xz} \\ -I_{xy} & ; & H \cos \theta \sin \phi & ; & -I_{yz} \\ -I_{xz} & ; & H \cos \theta \cos \phi & ; & I_z \end{vmatrix}$$

$$D_3 = \begin{vmatrix} I_x & ; & -I_{xy} & ; & -H \sin \theta \\ -I_{xy} & ; & I_y & ; & H \cos \theta \sin \phi \\ -I_{xz} & ; & -I_{yz} & ; & H \cos \theta \cos \phi \end{vmatrix}$$

We now express the angular velocities in terms of gimbal angles and rates:

$$\begin{aligned} p &= \dot{\phi} - \dot{\psi} \sin \theta \\ q &= \dot{\theta} \cos \phi + \dot{\psi} \cos \theta \sin \phi \\ r &= -\dot{\theta} \sin \phi + \dot{\psi} \cos \theta \cos \phi \end{aligned} \tag{7}$$

Or, solving for ϕ , θ , and ψ , we get

$$\begin{aligned}\dot{\phi} &= p + \dot{\psi} \sin \theta \\ \dot{\theta} &= q \cos \phi - r \sin \phi \\ \dot{\psi} \cos \theta &= q \sin \phi + r \cos \phi\end{aligned}\tag{8}$$

Finally, introducing (6) into (8), we get

$$\begin{aligned}D\dot{\phi} &= D_1 + (D_2 \sin \phi + D_3 \cos \phi) \tan \theta \\ D\dot{\theta} &= D_2 \cos \phi - D_3 \sin \phi \\ D\dot{\psi} \cos \theta &= D_2 \sin \phi + D_3 \cos \phi\end{aligned}\tag{9}$$

Equations (9) describe the attitude of a body with an angular impulse. This system of first-order differential equations can be simplified if we choose a particular body-fixed coordinate system that is aligned with the principal axes ξ , η , ζ . The inertia tensor \tilde{I} can then be expressed by a diagonal matrix:

$$\tilde{I} = \begin{bmatrix} I_\xi & 0 & 0 \\ 0 & I_\eta & 0 \\ 0 & 0 & I_\zeta \end{bmatrix}\tag{10}$$

and equations (5) simplify to

$$\begin{aligned}\Omega_\xi I_\xi &= -H \sin \vartheta \\ \Omega_\eta I_\eta &= H \cos \vartheta \sin \varphi \\ \Omega_\zeta I_\zeta &= H \cos \vartheta \cos \varphi\end{aligned}\tag{11}$$

Rewriting (8) in our new notation,

$$\begin{aligned}\dot{\mathcal{J}} &= \Omega_{\eta} \cos \varphi - \Omega_{\zeta} \sin \varphi \\ \dot{\varphi} &= \Omega_{\zeta} + \dot{\mathcal{J}} \sin \mathcal{J} \\ \dot{\mathcal{J}} \cos \mathcal{J} &= \Omega_{\eta} \sin \varphi + \Omega_{\zeta} \cos \varphi\end{aligned}\tag{12}$$

Finally, we get

$$\begin{aligned}\dot{\mathcal{J}} &= \frac{H}{2} \left(\frac{1}{I_{\eta}} - \frac{1}{I_{\zeta}} \right) \cos \mathcal{J} \sin 2\varphi \\ \dot{\varphi} &= H \left(\frac{\sin^2 \varphi}{I_{\eta}} + \frac{\cos^2 \varphi}{I_{\zeta}} \right) \\ \dot{\varphi} &= H \left(-\frac{1}{I_{\zeta}} + \left(\frac{\sin^2 \varphi}{I_{\eta}} + \frac{\cos^2 \varphi}{I_{\zeta}} \right) \right) \sin \mathcal{J}\end{aligned}\tag{13a}$$

or, using

$$\begin{aligned}\cos^2 \varphi &= \frac{1}{2} + \frac{1}{2} \cos 2\varphi \\ \sin^2 \varphi &= \frac{1}{2} - \frac{1}{2} \cos 2\varphi\end{aligned}$$

we get

$$\begin{aligned}\dot{\mathcal{J}} &= \frac{H}{2} \left(\frac{1}{I_{\eta}} + \frac{1}{I_{\zeta}} \right) + \frac{H}{2} \left(\frac{1}{I_{\zeta}} - \frac{1}{I_{\eta}} \right) \cos 2\varphi \tag{13b} \\ \dot{\varphi} &= \frac{H}{2} \left(-\frac{2}{I_{\zeta}} + \frac{1}{I_{\eta}} + \frac{1}{I_{\zeta}} + \left(\frac{1}{I_{\zeta}} - \frac{1}{I_{\eta}} \right) \cos 2\varphi \right) \sin \mathcal{J} \tag{13c}\end{aligned}$$

For rotational symmetry ($I_\eta = I_\zeta$) we get

$$\mathcal{J}, \dot{\varphi}, \dot{\psi} = \text{Const.}$$

and

$$\begin{aligned} L_z &= \text{const} \\ L_\eta &= A \sin \varphi \\ L_\zeta &= A \cos \varphi \end{aligned}$$

These equations describe the nutational motion of a cylinder of perfect rotational symmetry. The length axis is moving on a circular cone with constant angular and roll velocity--a well-known phenomenon.

Let us now consider the case of a body with near rotational symmetry around the length axis and small angle \mathcal{J} :

$$\begin{aligned} I_\zeta - I_\eta &= \Delta I \ll I_\zeta \\ \mathcal{J} &\ll \varphi \end{aligned}$$

and

$$\begin{aligned} \dot{\mathcal{J}} &\approx \frac{1}{2} \frac{H \Delta I}{I_\zeta^2} \sin 2\varphi \\ \dot{\varphi} &\approx -H \left(\frac{1}{I_\zeta} - \frac{1}{I_\eta} \right) \mathcal{J} \\ \dot{\psi} &\approx \frac{H}{I_\zeta} \end{aligned}$$

Combining the first and last of these equations, we eliminate \mathcal{J} and get

$$\ddot{\varphi} = - \frac{1}{2} \left(\frac{1}{I_z} - \frac{1}{I_y} \right) \frac{H^2}{I_y} \Delta I \sin 2\varphi \quad (14)$$

i. e. , the equation for the mathematical pendulum. For ΔI positive the rotation around the ζ axis is stable and for ΔI negative the rotation around the η axis is stable, the period T increasing with decreasing ΔI .

B. EFFECT OF MASS MOTION WITHIN THE SYSTEM

Next, how does a change in the mass distribution inside the station affect the motion of the station? The total angular impulse does not change because the mass motion is a result of internal forces. Nor does the center of mass move. But the origin of the body-fixed coordinate system does move and the inertia tensor changes. In addition, we must remember that the angular momentum varies with location. A mass close to the center of rotation has less angular momentum than a mass located farther out. Thus a mass that moves away from the center of rotation is accelerated, thereby slowing the part of the station it moves to.

Let us assume that a mass m moves from $\bar{\rho}_0$ to $\bar{\rho}$ inside the station. Although the position vector of the center of mass in the space-fixed coordinate system does not change, the location \bar{R} of the center of gravity in the body-fixed coordinate system does move. Initially, we have

$$\sum_{m_i \neq m} m_i \bar{g}_i + m \bar{g}_0 = 0$$

With m moved to $\bar{\rho}$ the center of gravity has moved to \bar{R} , given by

$$\begin{aligned} M \cdot \bar{R} &= \sum_{m_i \neq m} m_i \bar{g}_i + m \bar{g} \\ &= m \bar{g} - m \bar{g}_0 \\ \bar{R} &= \frac{m}{M} (\bar{g} - \bar{g}_0) \end{aligned} \tag{15}$$

where M is the total mass of the system.

The angular impulse \bar{H} , which remains unchanged, is given by

$$\bar{H} = \sum_{\text{all } m} m_i \bar{r}_i \times \bar{v}_i$$

with \bar{r}_i the position vector of m_i and \bar{v}_i the velocity of m_i (relative to the center of mass) measured in space-fixed coordinates.

We write the equation for the angular impulse in body-fixed coordinates:

$$\bar{r}_i = \bar{g}_i - \bar{R}$$

$$\begin{aligned} \bar{v}_i &= \frac{d}{dt}(\bar{r}_i) = \dot{\bar{r}}_i + \bar{\Omega} \times \bar{r}_i \\ &= \dot{\bar{g}}_i - \dot{\bar{R}} + \bar{\Omega} \times (\bar{g}_i - \bar{R}) \end{aligned}$$

$$\bar{H} = \sum m_i (\bar{g}_i - \bar{R}) \times (\dot{\bar{g}}_i - \dot{\bar{R}}) + \sum m_i (\bar{g}_i - \bar{R}) \times \bar{\Omega} \times (\bar{g}_i - \bar{R})$$

Using the formula $\bar{a} \times (\bar{b} \times \bar{c}) = \bar{b}(\bar{a} \cdot \bar{c}) - \bar{c}(\bar{a} \cdot \bar{b})$, we get

$$\begin{aligned} \bar{H} &= \sum m_i (\bar{g}_i - \bar{R}) \times \dot{\bar{g}}_i - \sum m_i (\bar{g}_i - \bar{R}) \times \dot{\bar{R}} + \bar{\Omega} \sum m_i (\bar{g}_i - \bar{R})^2 \\ &\quad - \sum m_i (\bar{g}_i - \bar{R}) \cdot (\bar{\Omega} \times (\bar{g}_i - \bar{R})) \end{aligned} \quad (16)$$

The first two terms show the effect of the mass motion; the last two terms, which depend only on the mass distribution, must correspond with equation (3). Evaluating the first two terms further, we note that because $\dot{\bar{p}}_1 = 0$ for all m_i except the moving mass m ,

$$\sum m_i (\bar{g}_i - \bar{R}) \times \dot{\bar{g}}_i = m(\bar{g} - \bar{R}) \times \dot{\bar{g}}$$

and, according to the definition of \bar{R} ,

$$\sum m_i (\bar{g}_i - \bar{R}) = 0$$

Therefore the second term equals zero:

$$\sum m_i (\bar{g}_i - \bar{R}) \times \dot{\bar{R}} = 0$$

The equation for the angular impulse is now

$$\bar{H} = m(\bar{g} - \bar{R}) \times \dot{\bar{g}} + \bar{\Omega} \cdot \tilde{I} \quad (17)$$

The x component of $\bar{\Omega} \cdot \tilde{I}$ (see equation 16) is given by

$$\begin{aligned} (\bar{\Omega} \cdot \tilde{I})_x &= p \sum m_i [(x_i - X)^2 + (y_i - Y)^2 + (z_i - Z)^2] - p \sum m_i (x_i - X)^2 \\ &\quad - q \sum m_i (x_i - X)(y_i - Y) - r \sum m_i (x_i - X)(z_i - Z) \\ &= p \sum m_i [(y_i - Y)^2 + (z_i - Z)^2] - q \sum m_i (x_i - X)(y_i - Y) \\ &\quad - r \sum m_i (x_i - X)(z_i - Z) \end{aligned}$$

and the other components of $\bar{\Omega} \cdot \tilde{I}$ have the corresponding form. We use these equations to evaluate the inertia tensor \tilde{I} :

$$\begin{aligned} \bar{I}_{xx} &= \sum m_i [(y_i - Y)^2 + (z_i - Z)^2] \\ &= \sum m_i (y_i^2 + z_i^2) - 2Y \sum m_i y_i - 2Z \sum m_i z_i + M(Y^2 + Z^2) \\ &= \bar{I}_{xx,0} - m(y_0^2 + z_0^2) + m(y^2 + z^2) - 2Y m(y - y_0) \\ &\quad - 2Z m(z - z_0) + M(Y^2 + Z^2) \end{aligned}$$

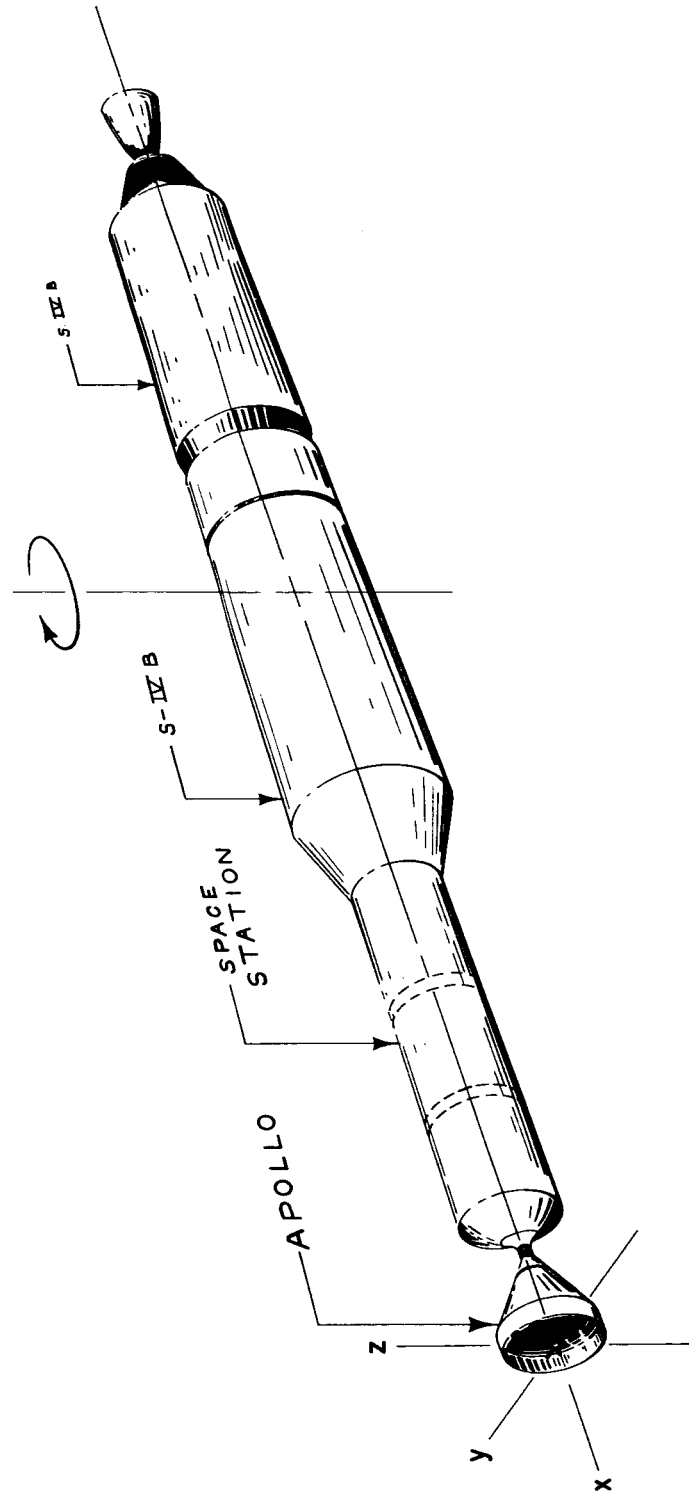


Figure 2. Model of Rotating Space Station

and (see equation 15)

$$I_x = I_{x_0} + m(y^2 - y_0^2) + m(z^2 - z_0^2) - \frac{m^2}{M}(y - y_0)^2 - \frac{m^2}{M}(z - z_0)^2 \quad (18a)$$

Since the body axes are the principal axes for $\rho = \rho_0$, we get

$$I_{xy} = m(x_0 y - x y_0) - \frac{m^2}{M}(x - x_0)(y - y_0) \quad (18b)$$

Similarly, we get

$$I_y = I_{y_0} + m(x^2 - x_0^2) + m(z^2 - z_0^2) - \frac{m^2}{M}(x - x_0)^2 - \frac{m^2}{M}(z - z_0)^2 \quad (18c)$$

$$I_z = I_{z_0} + m(x^2 - x_0^2) + m(y^2 - y_0^2) - \frac{m^2}{M}(x - x_0)^2 - \frac{m^2}{M}(y - y_0)^2 \quad (18d)$$

$$I_{xz} = m(xz - x_0 z_0) - \frac{m^2}{M}(x - x_0)(z - z_0) \quad (18e)$$

$$I_{yz} = m(yz - y_0 z_0) - \frac{m^2}{M}(y - y_0)(z - z_0) \quad (18f)$$

Equations (17) and (18) describe the dynamics of a rotating space station with no external torques.

For our numerical evaluation of equations (15), (17), and (18), we have used a model of a space station similar to one proposed in a study conducted by the MSFC Propulsion and Vehicle Engineering Laboratory at the request of the MSFC Future Projects Office (Figure 2). The station is nearly cylindrical and rotates around its axis of maximum moment of inertia. The rate of rotation, Ω , is 0.628 rad/sec and the crew compartment extends 12 to 18 meters from the center of rotation. The resulting artificial gravity, $\Omega^2 \cdot r$

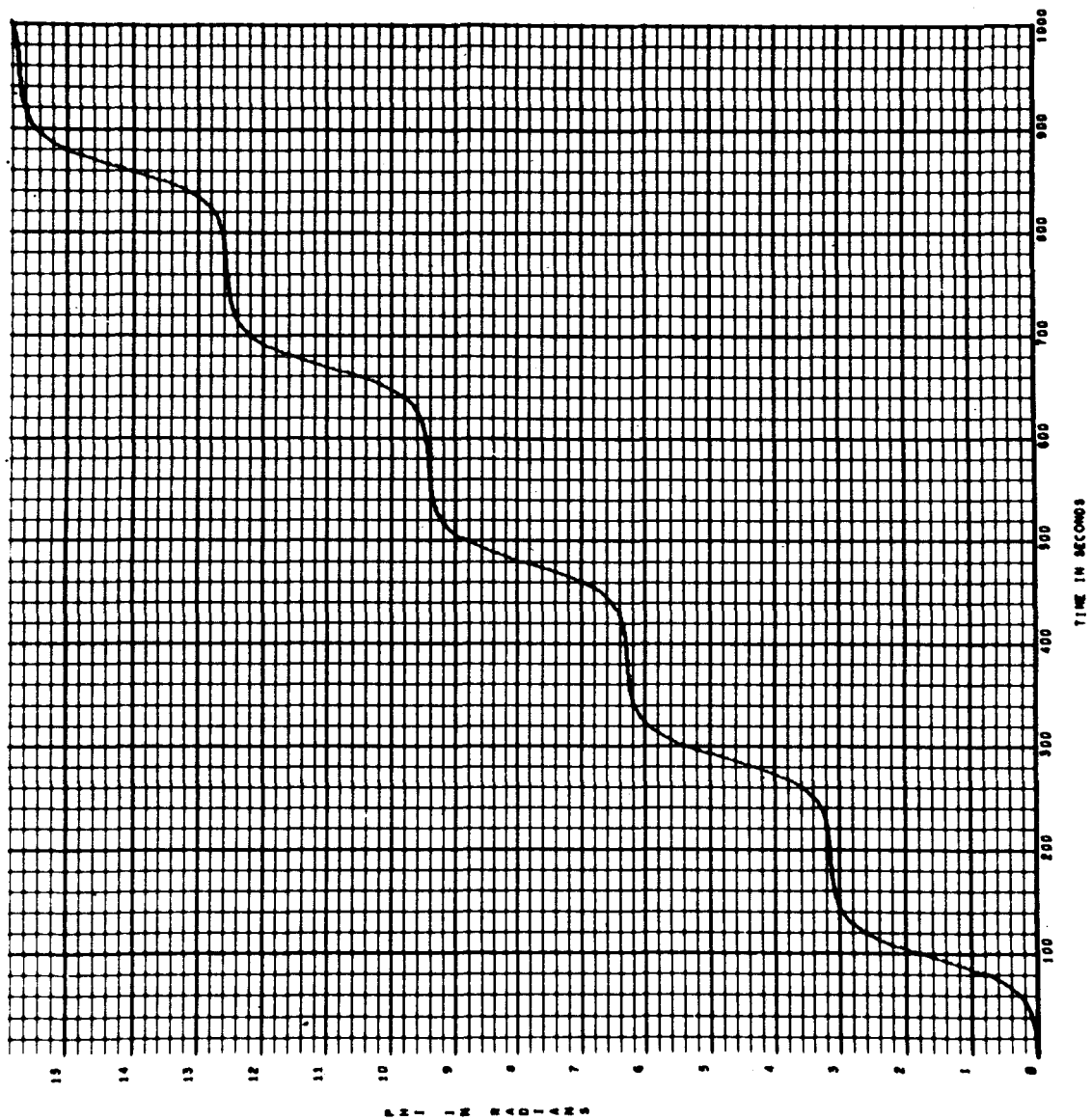


Figure 3a. ϕ Response of Station (Given Rotational Symmetry Around Length Axis) to Mass Motion from $x = 15\text{m}$, $z = 0$ to $x = 15\text{m}$, $z = 1.8\text{m}$

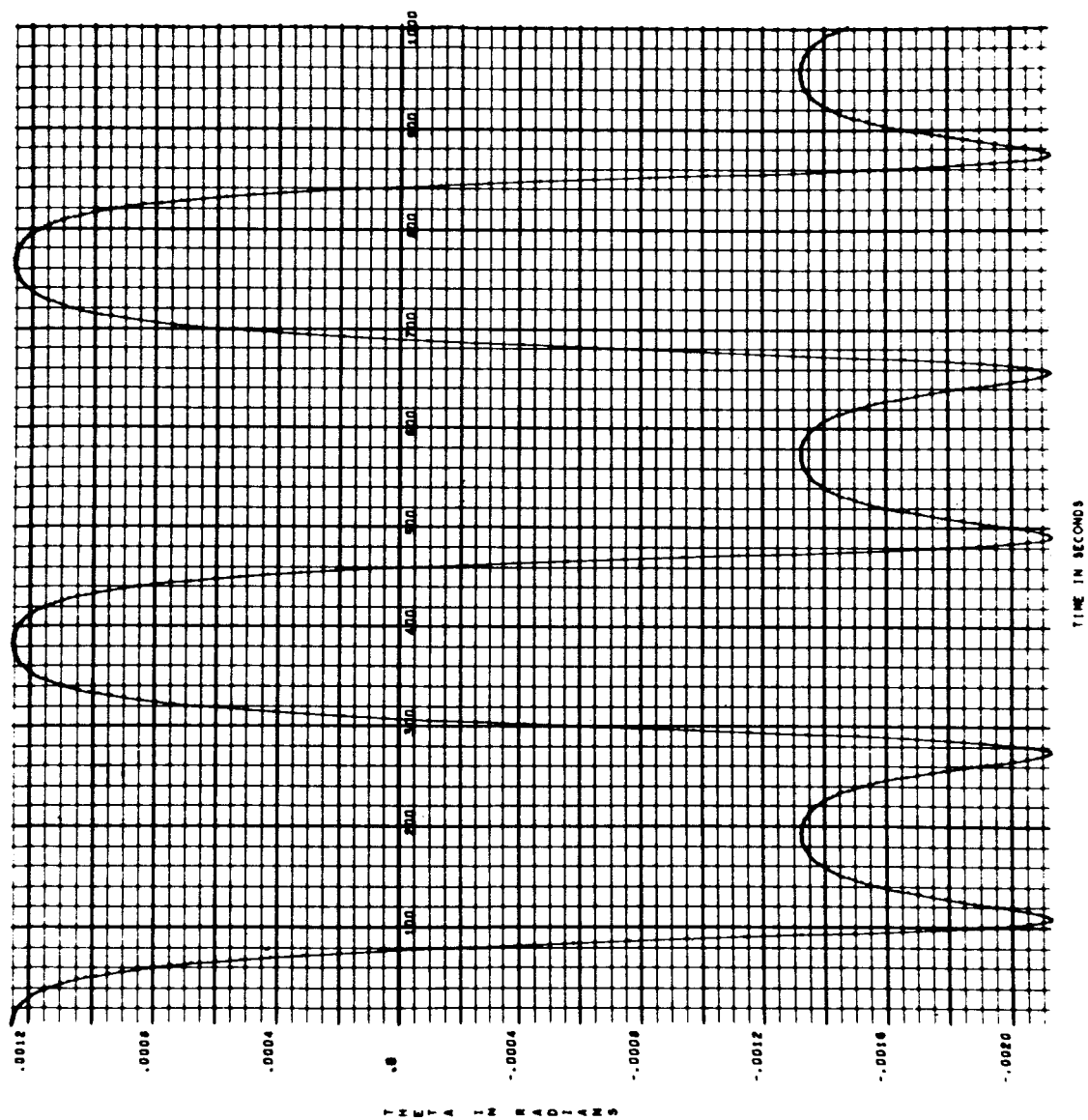


Figure 3b. θ Response of Station (Given Rotational Symmetry Around Length Axis) to Mass Motion from $x = 15\text{m}$, $z = 0$ to $x = 15\text{m}$, $z = 1.8\text{m}$

ranges from 0.48 g to 0.72 g. Three astronauts weighing 90 kilograms each are free to move about in this area. The maximum moment of inertia, I_z , is 6,000,000 kg m². The moment of inertia around the length axis, I_x , is 112,000 kg m².

Several different mass motions were studied. Our study showed that a station with rotational symmetry around the length axis responds to mass disturbances, both small and large, with large roll motions. This is demonstrated on Figure 3, which shows the results of a digital evaluation. A continuous roll motion is produced in response to a mass motion from $x = 15$ m, $z = 0$ m to $x = 15$ m, $z = 1.8$ m. The deflection in θ is negligible. (The deflection in θ consists of a component proportional to $\cos \phi$ and, according to equation (13c), superimposed on this a component proportional to $\dot{\phi}$. The component proportional to $\cos \phi$ is caused by the angle between the principal axis ξ and the body axis x .) The mass motion converts the z axis into an axis of intermediate moment of inertia, the rotation around this axis is unstable, and because the motion (the distance of m from the center of rotation increases) introduces a small positive initial roll velocity, the roll motion is continuous.

But even as little as 0.2% asymmetry (i. e., the asymmetry of the model used in our numerical evaluation) is sufficient to insure that the roll deflection in response to a single motion is limited to less than 10°. However, because of the absence of damping, whether or not a new mass motion will increase or decrease an existing oscillation depends on the timing of the new mass motion. (See the discussion of cancellation of roll by motion of the astronauts, pg. 28.)

Another disturbance that can be considered is the effect of rotating machinery (generators, pumps, etc.) on board the station. We modify equation (17) to include the effect of rotating machinery with body-fixed axes:

$$\bar{H} = m(\bar{g} - \bar{R}) \times \dot{\bar{g}} + \bar{\Omega} \cdot \bar{I} + \bar{h} \quad (19)$$

where \bar{h} is the angular impulse of the rotating machinery. Written in components, equation (19) becomes

$$\begin{aligned}
 -H \sin \theta &= h_x + p I_{xx} - q I_{xy} - r I_{xz} + m[(y-Y)\dot{z} - (z-Z)\dot{y}] \\
 H \cos \theta \sin \phi &= h_y - p I_{xy} + q I_{yy} - r I_{yz} + m[(z-Z)\dot{x} - (x-X)\dot{z}] \\
 H \cos \theta \cos \phi &= h_z - p I_{xz} - q I_{yz} + r I_{zz} + m[(x-X)\dot{y} - (y-Y)\dot{x}]
 \end{aligned}$$

We see from these equations that flywheels can enforce the correct attitude in the steady state, in spite of mass displacements.

In the steady state, with p, q, \dot{x}, \dot{y} , and $\dot{z} = 0$, ϕ and θ can be reduced to zero if

$$\begin{aligned}
 h_x &= r I_{xz} \\
 h_y &= r I_{yz}
 \end{aligned}$$

We can determine the required angular impulses to do this for the maximum possible values of I_{xz} and I_{yz} :

$$I_{xz} = mxz = 270 \text{ kg} \cdot 1.8 \text{ m} \cdot 1.8 \text{ m} = 8,750 \text{ kg m}^2$$

$$I_{yz} = myz = 270 \text{ kg} \cdot 1.27 \text{ m} \cdot 1.27 \text{ m} = 435 \text{ kg m}^2$$

Because the roll deflection is considerably larger than the pitch deflection, it is more important to reduce roll. Fortunately, this requires a twenty times smaller angular impulse. Moreover, because a deflection in the roll orientation is less disturbing to the astronauts than a roll oscillation, only methods of limiting roll oscillation were studied. Two methods were studied in detail: controlled motion of the astronauts and automatic control by flywheels.

To simplify our analysis of the effect of rotating machinery with body-fixed axes, we shall assume that the body-fixed axes are the principal axes and that the astronauts are at rest. Equations (19) then become

$$-H \sin \theta = h_x + p I_x$$

$$H \cos \theta \sin \phi = h_y + q I_y$$

$$H \cos \theta \cos \phi = h_z + r I_z$$

The magnitude of h_x that can be tolerated is determined by the transients it introduces into roll during starting and stopping.

We can estimate the initial roll velocity caused by a fast start (assuming that $\theta = 0$ initially) from

$$I_x p + h_x = 0 = h_x + I_x \dot{\phi}_0$$

If we limit the roll deflection to a maximum of 0.1 rad, the roll oscillation will be approximately sinusoidal, with the relation between the maximum angular velocity and the angular deflection given by

$$\phi_m = \frac{I}{2\pi} \dot{\phi}_0$$

It follows that

$$|h_x| < \frac{I_x \cdot 2\pi}{T} \cdot 0.1 \text{ rad} = 1850 \text{ kg m}^2 \text{ sec}^{-1}$$

This angular impulse causes a deflection in θ after the roll oscillation is damped out:

$$\begin{aligned} \theta &= -\frac{h_x}{H} = \frac{1850}{6,000,000 \cdot 0.628} \\ &= -0.5 \cdot 10^{-3} \text{ rad} \end{aligned}$$

But, because of their small size, θ and $\dot{\theta}$ can be neglected and we get for the components of Ω :

$$q = \dot{\psi} \cos \theta \sin \phi \quad r = \dot{\psi} \cos \theta \cos \phi$$

Using these expressions, we get

$$h_z = (H - \dot{\psi} I_2) \cos \theta \cos \phi$$

or

$$\dot{\psi} \approx \frac{H - h_z}{I_2}$$

Thus, because H is very large, the change in $\dot{\psi}$ resulting from rotating machinery with its axis parallel to z can be neglected.

Finally, for h_y , we get

$$h_y \approx H \left(1 - \frac{I_y}{I_z}\right) \cos \theta \sin \phi$$

Hence an angular impulse h_y causes a steady state deflection in ϕ . Imposing the same limit on the steady state deflection as we did on the roll oscillation, we get

$$\begin{aligned} h_y &< H \left(1 - \frac{I_y}{I_z}\right) \cdot 0.1 \\ &< 6,000,000 \cdot 0.002 \cdot 0.628 \cdot 0.1 \\ &< 750 \text{ kg m}^2 \text{ sec}^{-1} \end{aligned}$$

In sum, then, rotating machinery interferes least with the dynamics of the rotating station when its axis is aligned with the z axis of the station.

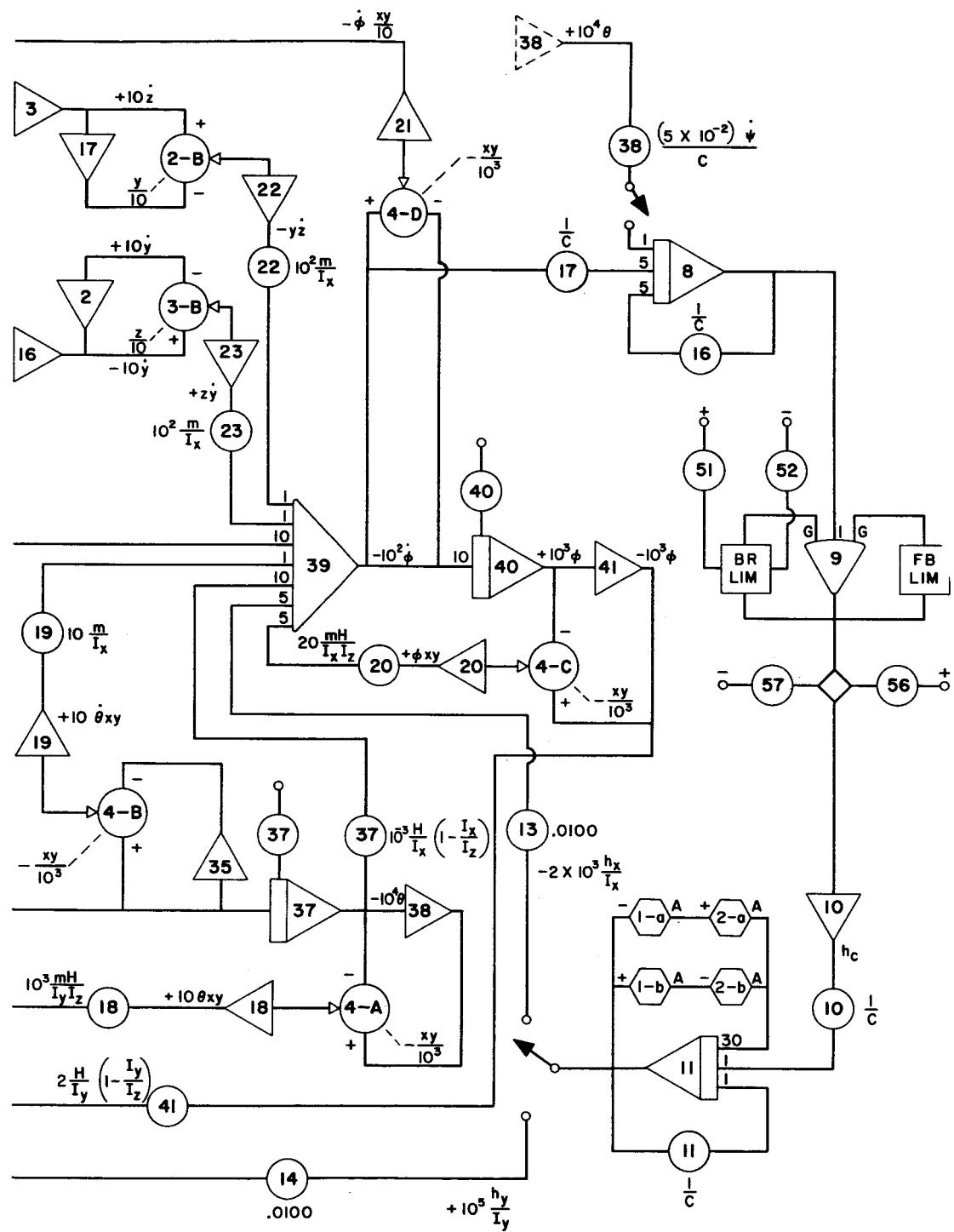


Figure 4. Analog Computer Program

SECTION III. NUMERICAL EVALUATION

A. THE ANALOG COMPUTER PROGRAM

To study the behavior of equation (19), we programmed it on an analog computer. The following simplifying assumptions were made: that $m \ll M$, that the position of m in the undisturbed system is at $y_0, z_0 = 0$, that changes in I_x, I_y, I_z resulting from mass displacements can be neglected, and that small angle approximations will have no significant effect on the results. We therefore get

$$\begin{aligned}
 I_{xy} &\approx mxy; \quad I_{yz} \approx myz; \quad I_{zx} \approx mxz \\
 p &\approx \dot{\phi} - \dot{\psi}\theta; \quad q \approx \dot{\theta} + \dot{\psi}\phi; \quad r \approx \dot{\psi} \approx \frac{H}{I_z} \\
 I_x \ddot{\phi} &\approx -H\left(1 - \frac{I_{xx}}{I_z}\right)\theta + mxy\ddot{\theta} + m\frac{H}{I_z}xy\dot{\phi} + m\frac{H}{I_z}xz \\
 &\quad + m(\dot{y}z - \dot{z}y) - h_x \\
 I_y \ddot{\theta} &\approx H\left(1 - \frac{I_{yy}}{I_z}\right)\phi + mxy\ddot{\phi} - m\frac{H}{I_z}xy\dot{\theta} + m\frac{H}{I_z}yz \\
 &\quad + m(x\dot{z} - z\dot{x}) - h_y
 \end{aligned} \tag{20}$$

The analog computer program is shown on Figure 4.

The effect of a mass displacement depends on the path and on the schedule of the displacement. Figure 5 shows the response of the station to the motion of three astronauts ($3 \cdot 90 \text{ kg} = 270 \text{ kg}$) from $\{12 \text{ m}, 0, 0\}$ to $\{18 \text{ m}, 0, 1.8 \text{ m}\}$ along three different paths:

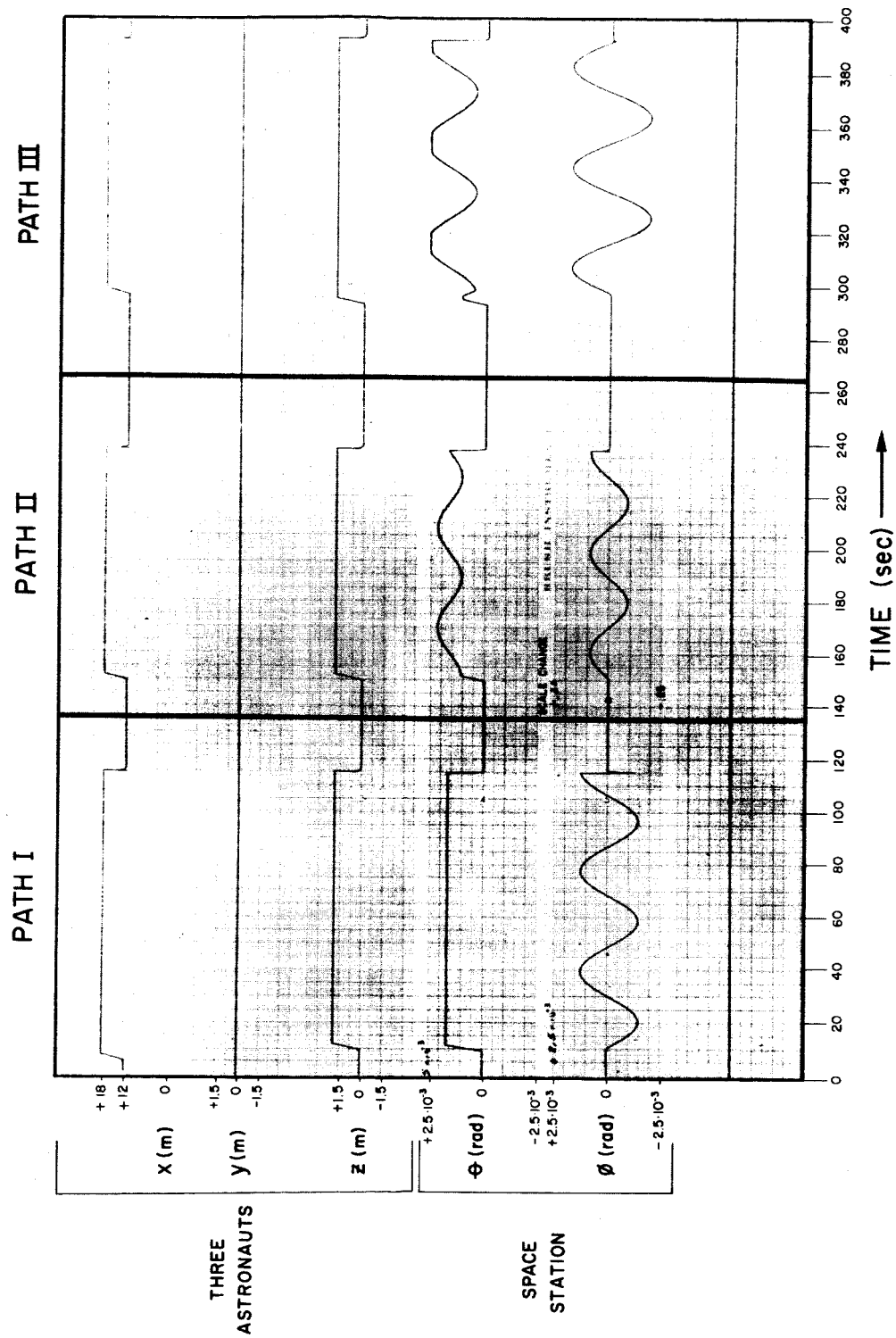


Figure 5. Response of Station to Motion in Unison of Three Astronauts from $\{12\text{m}, 0, 0\}$ to $\{18\text{m}, 0, 1.8\text{m}\}$ along Three Different Paths. (Note 100-to-One Scale Change in ϕ between Path I and Paths II and III.)

Path I. From $\{12\text{m}, 0, 0\}$ to $\{18\text{m}, 0, 0\}$ and then to $\{18\text{m}, 0, 1.8\text{m}\}$

Path II. From $\{12\text{m}, 0, 0\}$ to $\{18\text{m}, 0, 1.8\text{m}\}$ and then to $\{18\text{m}, 0, 1.8\text{m}\}$

Path III. From $\{12\text{m}, 0, 0\}$ to $\{12\text{m}, 0, 1.8\text{m}\}$ and then to $\{18\text{m}, 0, 1.8\text{m}\}$

Check runs on a digital computer show good agreement, indicating that the approximations used have no significant effect on the results. It follows from equation (13a) that the pitch amplitude is 0.007 of the roll amplitude. This too is in agreement with the computer results. The steady state pitch deflection can be determined from equation (E) of the Appendix, where the orientation of the principal axes of the space station relative to the body-fixed axes is described.

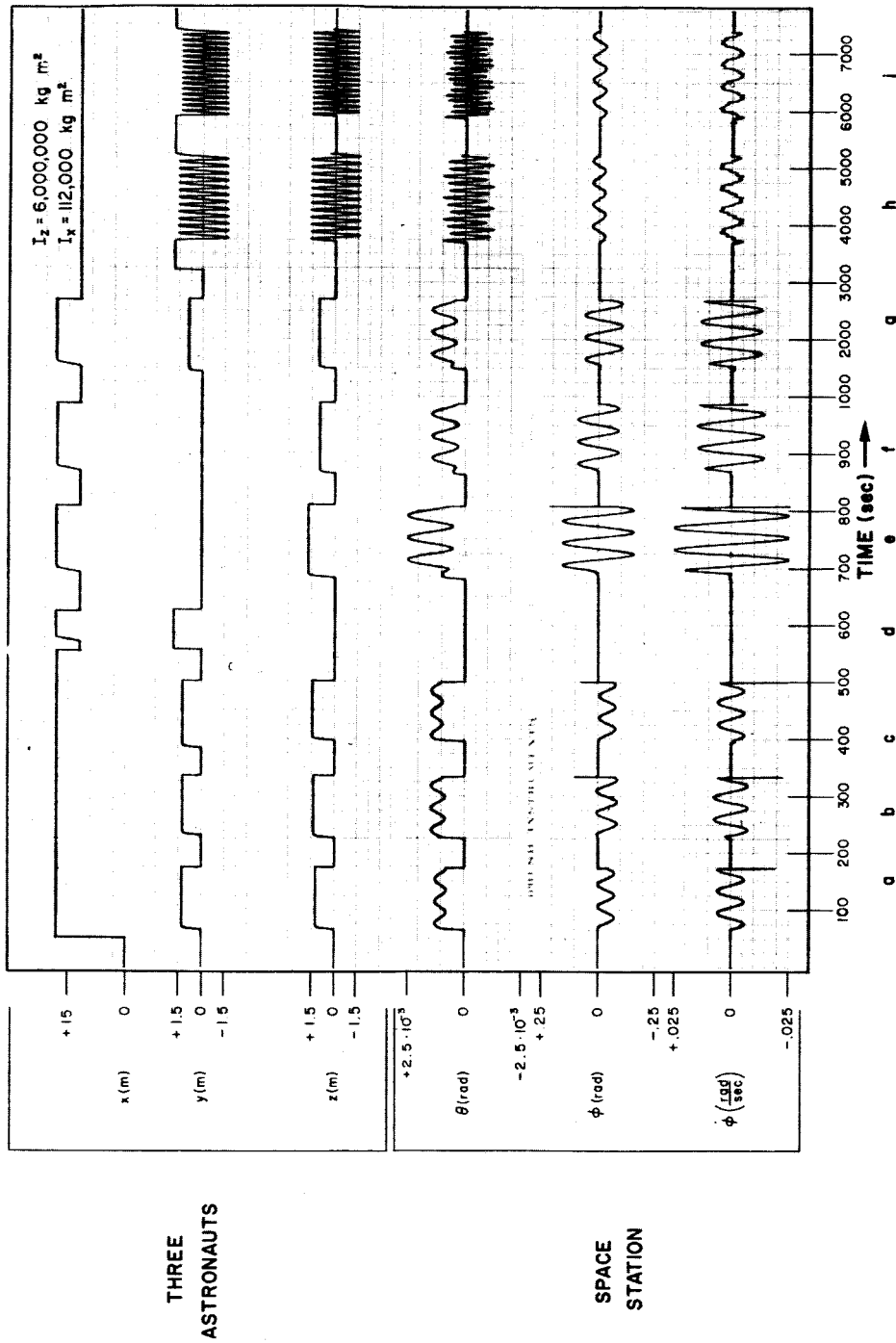


Figure 6. Response of Station to Motion in Unison of Three Astronauts (a-c) in yz Plane, (c, d) in xy Plane, (e-g) Parallel to but Not Along x Axis, (h, i) in Circle in yz Plane

B. EFFECT OF ASTRONAUTS' MOTION

The walking speed was assumed to be 0.9 m/sec. To simulate changes in velocity realistically, a first-order lag with a time constant of one second was added to the velocity term.

Motion in the yz plane, for example the motion of three astronauts from {18m, 0, 0} to {18m, 1.2m, 1.2m}, changes the direction of the principal axes η , ζ relative to the body axes and causes a roll oscillation, but the deflection in this case is only 2° . If this transfer occurs in two phases, for example from {18m, 0, 0} to {18m, 0, 1.2m} and then to {18m, 1.2m, 1.2m}, a small initial roll velocity ($+2.5 \cdot 10^{-3}$ rad/sec) is introduced in the second phase. The same two-phase transfer in a different sequence, i.e., from {18m, 0, 0} to {18m, 1.2m, 0} and then to {18m, 1.2m, 1.2m}, produces a small initial roll velocity of the opposite sign.

Because starting and stopping occur in time intervals that are small compared with the period of the oscillation, the effect of these on the roll amplitude can be neglected (Figure 6a-c).

Motion in the xy plane causes no roll, as can be seen on Figure 6c, d. The ladder for going from a lower to an upper deck of the spacecraft should therefore be located in the xy plane.

Motion parallel to, but not along, the x axis (constant $z \neq 0$) introduces large roll disturbances, mainly because of the change in angular momentum with distance from the center of rotation. The transfer of this momentum to the roll axis depends only on z , i.e., the torque generated by the Coriolis force (Figure 6e-g).

Walking in a circle in the yz plane (Figure 6h, i) introduces two disturbances: the attitude of the principal axes relative to the body axes is varied and an angular roll impulse is introduced. The first disturbance has a period corresponding to the time it takes to walk around half the circumference of the cylindrical station. Its effect can be seen in ϕ . The second disturbance is the reaction of the station to the initiation of circular motion by the astronauts. The

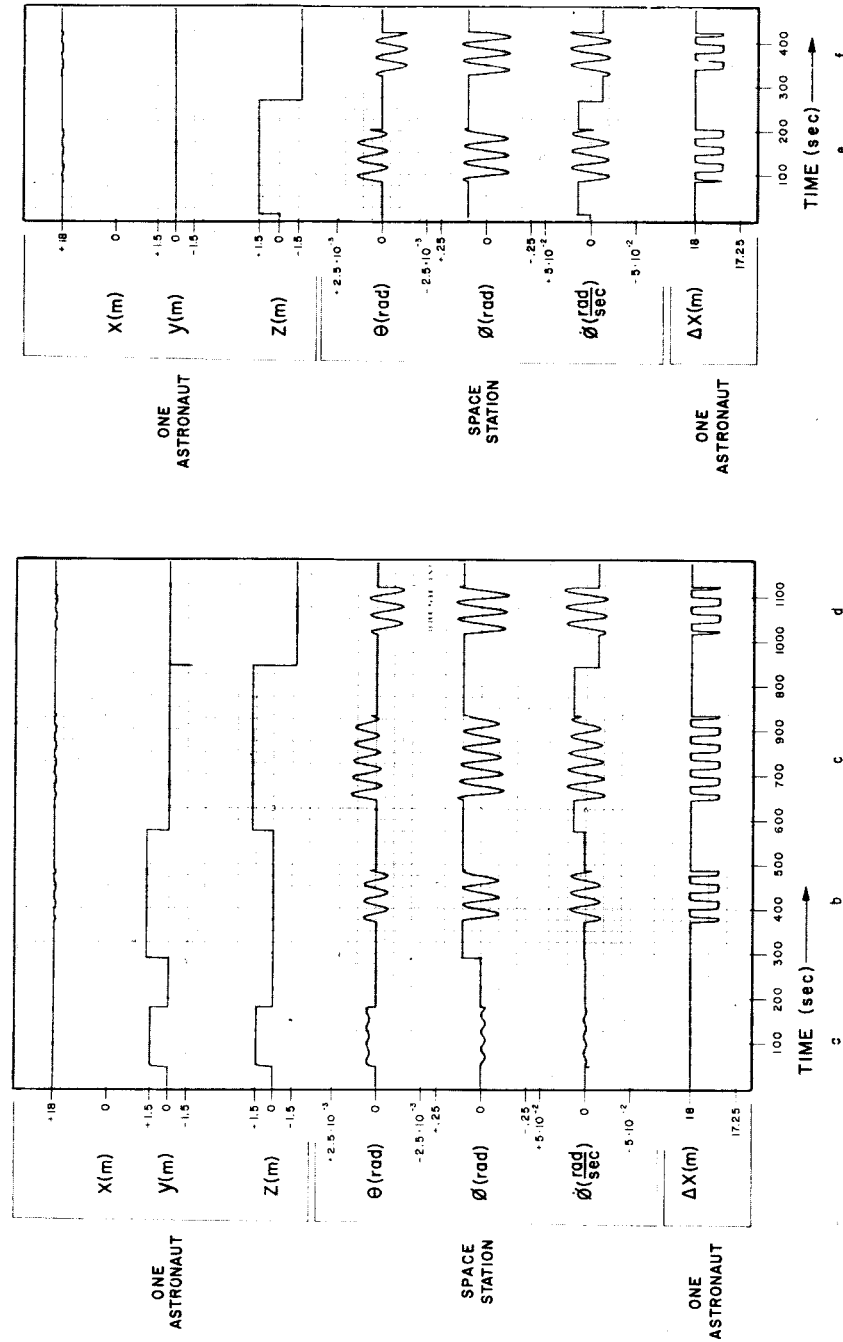


Figure 7. Effect of One Astronaut Moving in x Direction Synchronously with Roll: (a) Rotation of Principal Axes by Transfer from {18m, 0, 0} to {18m, 1.27m, 1.27m}, (b) Roll Unaffected by Motion in xy Plane, (c) Damping of Roll (Positive z), (d) Augmentation of Roll (Negative z), (e, f) Roll Unaffected by Motion in Phase with $\dot{\phi}$

initial roll velocity that results is given by

$$I_{xx} \dot{\phi}_0 = m g \cdot v = 270 \text{ kg} \cdot 1.8 \text{ m} \cdot 0.9 \text{ m/sec.}$$

The amplitude of the resultant roll (T = the period of the roll motion) is

$$\phi = \frac{\dot{\phi}_0 \cdot T}{2\pi} = 24 \cdot 10^{-3} \text{ rad}$$

All these disturbances are moderate. The roll angle never exceeds 10° . However, whether the roll of the spacecraft is increased or decreased depends on the phase of the recurrence of a disturbance.

Figure 7 shows the effect of one astronaut walking synchronously with a roll oscillation. Whether the effect is one of buildup or of decay depends on the phase relation. Hence it should be feasible to use the astronauts for corrective action to counteract roll of the spacecraft. Figure 7 shows the effect of motion in the x direction. Figure 7a repeats the effect of rotation of the principal axes by the transfer of one astronaut from $\{18 \text{ m}, 0, 0\}$ to $\{18 \text{ m}, 1.27 \text{ m}, 1.27 \text{ m}\}$. Figure 7b shows again that motion in the xy plane does not affect roll. Figure 7c shows a damping effect (positive z); Figure 7d shows an augmentation (negative z) for motion in the x direction in phase with ϕ ; Figure 7e, f shows that motion in the x direction in phase with $\dot{\phi}$ has no effect.

A more effective and convenient way to reduce a roll oscillation is shown on Figure 8a-g. Here the motion is parallel to, but not along, the y axis (constant $z \neq 0$) or parallel to, but not along, the z axis (constant $y \neq 0$) in phase with the roll velocity¹. The same motion in the opposite phase causes a buildup.

¹Measured as $\dot{\phi}$, i. e., as the gimbal rate of the inertial platform, or as p by a rate gyro mounted on the frame of the space station.

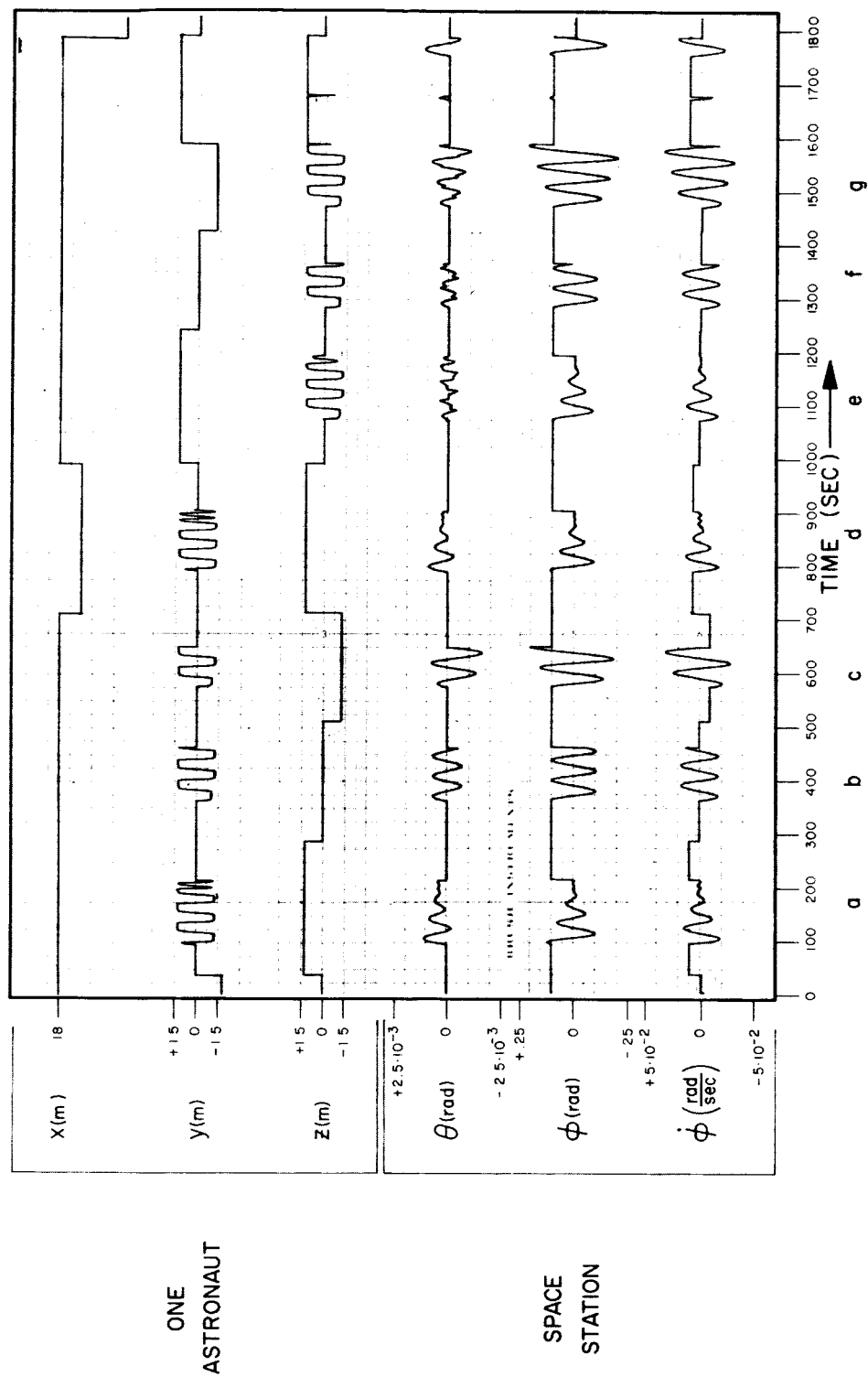


Figure 8. Correction of Initial Roll Disturbance by Controlled Motion of One Astronaut in yz Plane

C. AUTOMATIC CONTROL OF STATION'S ROLL MOTION

As already mentioned, properly controlled variations in flywheel rates could be used to damp out roll oscillations. We shall first consider the effect of a flywheel with its axis parallel to the x axis.

For simplicity, we assume that $I_{xy}, I_{yz}, I_{zx} = 0$ and that the astronauts are not moving. The station has a roll oscillation introduced by some previous disturbance. We use small angle approximations and equation (19) becomes, with $I_z - I_y = \Delta I$ and $I_z \gg \Delta I$,

$$\begin{aligned} -H\theta &\approx h_x + pI_x & p &\approx \dot{\phi} - \dot{\psi}\theta \\ H\phi &\approx qI_y & q &\approx \dot{\theta} + \dot{\psi}\phi \\ H &\approx rI_z & r &\approx \dot{\psi} \end{aligned}$$

Thus

$$\begin{aligned} \ddot{\phi} &\approx -H\left(\frac{1}{I_x} - \frac{1}{I_z}\right)\dot{\theta} - \frac{\dot{h}_x}{I_x} \\ \dot{\theta} &\approx \frac{\Delta I}{I_z} r\phi \end{aligned}$$

and

$$\ddot{\phi} \approx -\frac{\Delta I}{I_x} r^2\phi - \frac{\dot{h}_x}{I_x} \quad (21)$$

This equation shows that only a rate of the angular impulse of the flywheel, h_x , generates a torque. Thus if \dot{h}_x can be varied synchronously with $\dot{\phi}$, the roll oscillation of the station can be damped. But h_x cannot be used to counteract a steady-state deflection in ϕ caused by I_{yz} . However, according to Figure 6a, the largest possible steady state deflection due to I_{yz} is only 2° .

Another possibility is to use a flywheel with its axis parallel to the y axis. Using the same approximations, we get

$$\ddot{\phi} \approx - \frac{\Delta I}{I_x} r^2 \phi + r \frac{\dot{h}_y}{I_x} \quad (22)$$

We now get a damped roll oscillation if the angular impulse of the flywheel, h_y , is varied synchronously with $-\dot{\phi}$. Comparing equations (21) and (22), we can see that for an equal damping effect

$$r h_y = \dot{h}_x$$

An effective schedule for h was found to be a linear increase with time followed by an instantaneous braking action. This can be seen on Figure 9. For this schedule h_x is related to $h_{x\max}$ as follows (T = the roll period):

$$\begin{aligned} h_{x\max} &= \dot{h}_x \cdot \frac{T}{2} = 19 \dot{h}_x = 19.0628 h_{y\max} \\ &= 12 h_{y\max} \end{aligned}$$

Control by varying h_y turns out to be considerably more effective. Figure 9 shows the performance of such a control system. No phase adjustments were made to optimize the control. The simulation

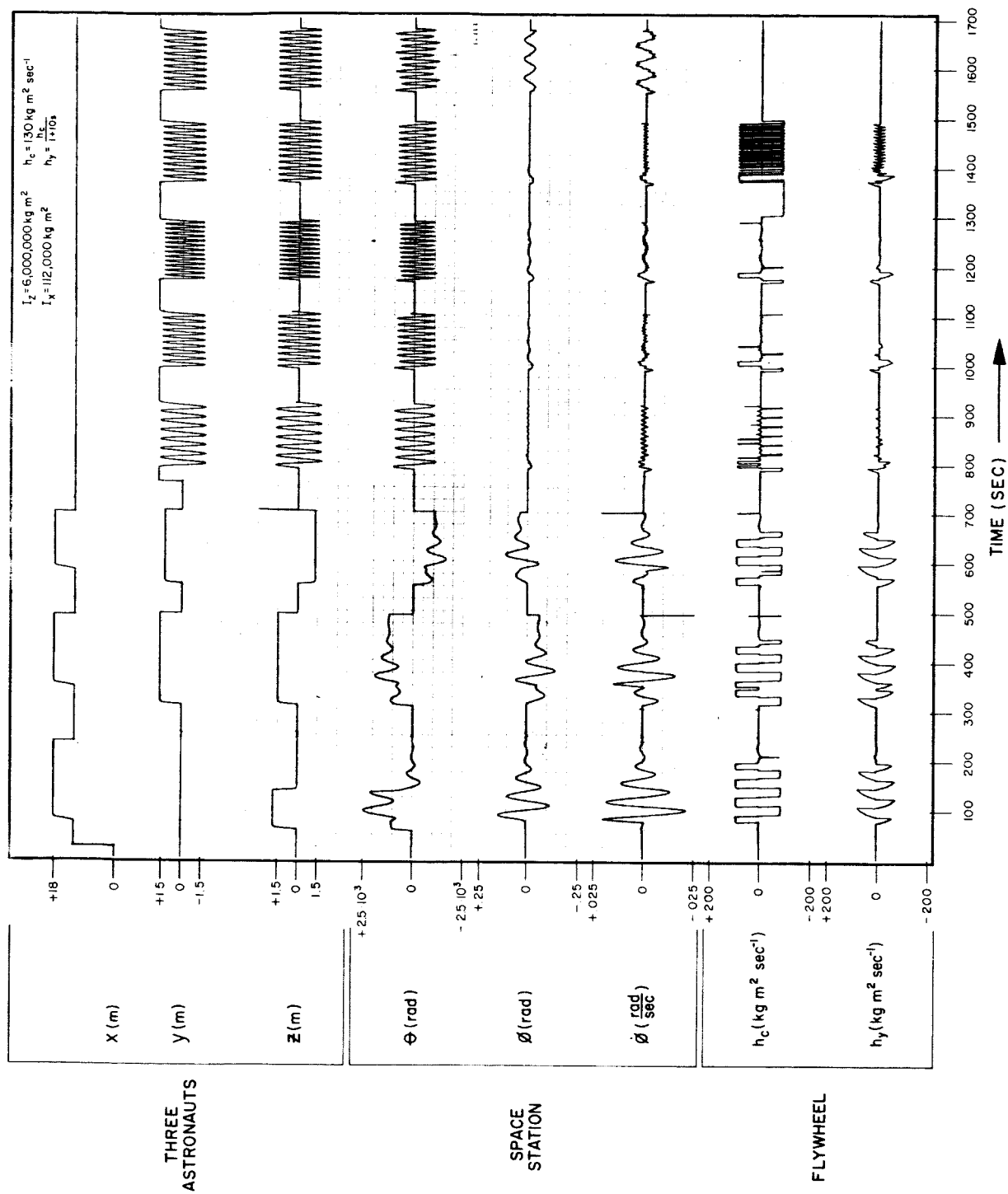


Figure 9. Correction of Initial Roll Disturbance by Flywheel Control System
(h_c = Angular Impulse of Flywheel)

assumes that the flywheel¹ is driven by a motor with a combined time constant of 10 seconds. (Therefore h_y does not remain constant, as was assumed above, but decays during the cycle.) The voltage applied to the motor is constant; only the polarity is controlled. Brakes are applied before the voltage is reversed. Thus

$$E = \text{const. sign } \dot{\phi} = c \cdot h_c$$

$$h_y = \frac{h_c}{1 + 10s}$$

The maximum required power, P , is half the maximum torque multiplied by half the maximum angular rate, i.e.,

$$P_{\max} = \frac{1}{4} \dot{h}_{\max} \cdot \frac{h_{\max}}{I_F}$$

With $I_F = 2 \text{ kg m}^2$ and $h_c = 100 \text{ lb ft sec}^{-1} = 130 \text{ kg m}^2 \text{ sec}^{-1}$, we get

$$P_{\max} = \frac{1}{4} \cdot \frac{130}{10} \cdot \frac{130}{2}$$

$$= 211 \text{ watt}$$

The maximum angular rate is therefore

$$\omega = \frac{130}{2} = 65 \text{ rad/sec}$$

$$= 620 \text{ rpm}$$

¹ A hydraulic system with circulating pump and valves could well be another feasible solution to the control system problem.

Or, rather than building up an angular impulse and then wasting the stored energy by braking, we can use a gimbal-mounted gyro with its axis aligned initially with the z axis (Figure 10). The required angular impulse, h_y , is generated by rotating the gimbal (its axis is parallel to the x axis) through an angle δ :

$$h_y = -I_s \dot{\Omega}_s \sin \delta$$

($I_s \cdot \Omega_s$ is the angular impulse of the spinning gyro.) The other two components of the angular impulse generated by this rotation are

$$h_x = I_{G,x} \dot{\delta}$$

$$h_z = I_s \dot{\Omega}_s \cos \delta$$

($I_{G,x}$ is the combined moment of inertia of the gimbal and the flywheel around the x axis.) Because it is small, the influence of these other two components on the motion of the station can be neglected.

The torque generated by turning the gimbal is

$$\begin{aligned} \vec{L} &= \dot{\vec{h}} + \vec{\Omega} \times \vec{h} \\ &= [I_{G,x} \ddot{\delta} + I_s \Omega_s (q \cos \delta + r \sin \delta)] \vec{i} \\ &\quad - [I_s \Omega_s \dot{\delta} \cos \delta + p I_s \Omega_s \cos \delta + r I_{G,x} \dot{\delta}] \vec{j} \\ &\quad - [I_s \Omega_s \dot{\delta} \sin \delta + p I_s \Omega_s \sin \delta + q I_{G,x} \dot{\delta}] \vec{k} \end{aligned}$$

The j and k components of L, along with the centrifugal forces, constitute the load on the gimbal -- and spin -- bearings. Sufficient power must be provided to replace the energy dissipated by friction.

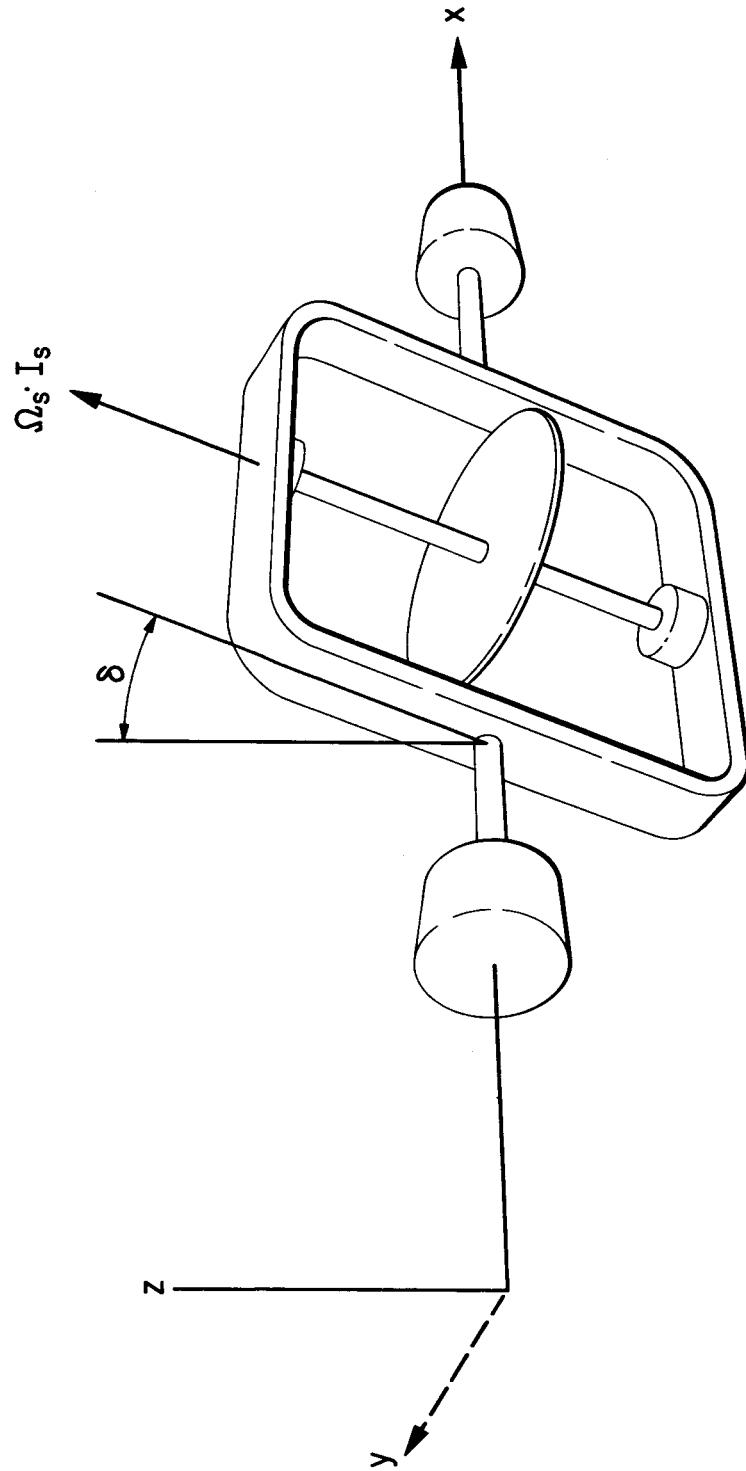


Figure 10. Stabilization by a Gyro

Because the station is rotating, $L_x \neq 0$. Power is therefore required to turn the gimbal:

$$P = L_H \cdot \dot{\delta}$$

This power builds up potential energy:

$$E = \int_0^{t(\delta)} L_H \dot{\delta} dt \approx \left[\frac{1}{2} I_{G_H} \dot{\delta}^2 \right]_{\dot{\delta}=0}^{\dot{\delta}=\dot{\delta}} + I_S \Omega_S \int_0^{\delta} r \sin \delta d\delta$$

(q is neglected as small) or, considering r to be independent of δ :

$$E \approx I_S \Omega_S r (1 - \cos \delta)$$

and for $\delta = \frac{\pi}{2}$,

$$E \approx 82 \text{ watt sec}$$

This energy has only to be built up. As soon as the torque is removed, the gimbal swings back to the opposite deflection.

It may be advantageous to use moderate rates of rotation of the gyro. The stored kinetic energy would thus be small, allowing the control to be switched on and the gyro to be started as required. The stored kinetic energy for an angular impulse, $I_S \cdot \Omega_S$, of $130 \text{ kg m}^2 \text{ sec}^{-1}$ is, given that $I_S = 2 \text{ kg m}^2$,

$$E = 4250 \text{ watt sec}$$

SECTION IV. EFFECT OF EXTERNAL TORQUES

Still to be mentioned are the effects of external torques. These have not been considered in our analyses mainly because external torques in space are small (gravity gradient, magnetic fields, radiation pressure, drag). They therefore change the angular impulse only very slowly:

$$L = \frac{dH}{dT}$$

The same can be said of the impact of meteoroids. Roll motion resulting from such impacts can be damped out as it occurs and the axis of rotation will be in line with the direction of the angular impulse.

Finally, it may occasionally be necessary to use jets to restore and maintain the desired rate of rotation and the direction in space of the axis of rotation.

SECTION V. CONCLUSIONS

Mass motion in a rotating space station of cylindrical shape causes the station to oscillate in the roll direction. The more nearly symmetrical the station is around its length axis, the larger the amplitude of the roll oscillation will be. But, as is shown by the example investigated, a difference even as small as 0.2% between the moments of inertia of the major and the intermediate axes suffices to keep the oscillation small. In addition, excessive roll can be reduced by control systems using a flywheel or corrective motion of the astronauts.

APPENDIX

ORIENTATION OF THE PRINCIPAL AXES OF THE SPACE STATION RELATIVE TO THE BODY-FIXED AXES

The angular impulse is related to the angular velocity by

$$\bar{H} = \begin{vmatrix} I_x & -I_{xy} & -I_{xz} \\ -I_{xy} & I_y & -I_{yz} \\ -I_{xz} & -I_{yz} & I_z \end{vmatrix} \cdot \bar{\Omega} \quad (A)$$

For \bar{H} pointing in the direction of the principal axis,

$$\bar{H} = \lambda \bar{\Omega}$$

Writing this in components,

$$\begin{aligned} I_x p - I_{xy} q - I_{xz} r &= \lambda p \\ -I_{xy} p + I_y q - I_{yz} r &= \lambda q \\ -I_{xz} p - I_{yz} q + I_z r &= \lambda r \end{aligned} \quad (B)$$

It follows that the determinant

$$\begin{vmatrix} (I_x - \lambda) & -I_{xy} & -I_{xz} \\ -I_{xy} & (I_y - \lambda) & -I_{yz} \\ -I_{xz} & -I_{yz} & (I_z - \lambda) \end{vmatrix} = 0$$

This cubic equation in λ has three roots, $\lambda_1, \lambda_2, \lambda_3$, which correspond to I_ξ, I_η, I_ζ . The value for λ closest to I_x is I_ξ . Using $\lambda_1 = I_\xi$, equations (B) become

$$\begin{aligned}(I_x - I_\xi)p - I_{xy}q - I_{xz}r &= 0 \\ -I_{xy}p + (I_y - I_\xi)q - I_{yz}r &= 0 \\ -I_{xz}p - I_{yz}q + (I_z - I_\xi)r &= 0\end{aligned}$$

The first equation can be interpreted as a scalar product $\bar{a} \cdot \bar{\Omega} = 0$ indicating that \bar{a} is perpendicular to $\bar{\Omega}$ with

$$\bar{a} = (I_x - I_\xi)\mathbf{i} - I_{xy}\mathbf{j} - I_{xz}\mathbf{k}$$

The second equation yields a vector, \bar{b} , with

$$\bar{b} = -I_{xy}\mathbf{i} + (I_y - I_\xi)\mathbf{j} - I_{yz}\mathbf{k}$$

The vector $\bar{a} \times \bar{b}$ has the direction of the principal axis ξ .

$$\bar{a} \times \bar{b} = \begin{vmatrix} \mathbf{i} & \mathbf{j} & \mathbf{k} \\ (I_x - I_\xi) & -I_{xy} & -I_{xz} \\ -I_{xy} & (I_y - I_\xi) & -I_{yz} \end{vmatrix}$$

We can now express the orientation of the principal axes relative to the body-fixed axes by determining the three Euler angles α, β, γ . We use the same sequence of rotation as we used in converting from the reference axes to the body-fixed axes. The z axis agrees with γ , the ξ axis with α . We can therefore use the matrix of equation (1):

$$\begin{bmatrix} p \\ q \\ r \end{bmatrix} = \begin{bmatrix} \cos\beta \cos\gamma & \cos\beta \sin\gamma & -\sin\beta \\ \cos\gamma \sin\beta \sin\alpha - \sin\gamma \cos\alpha & \sin\alpha \sin\beta \sin\gamma + \cos\alpha \cos\gamma & \sin\alpha \cos\beta \\ \cos\alpha \sin\beta \cos\gamma + \sin\alpha \sin\gamma & \cos\alpha \sin\beta \sin\gamma - \sin\alpha \cos\gamma & \cos\alpha \cos\beta \end{bmatrix} \begin{bmatrix} p \\ q \\ r \end{bmatrix} \quad (C)$$

Because $\bar{a} \times \bar{b}$ has the direction of the ξ axis, its component $i \cdot \bar{a} \times \bar{b}$ is proportional to $\cos \gamma \cos \beta$ and its component $j \cdot \bar{a} \times \bar{b}$ is proportional to $\sin \gamma \cos \beta$. We determine γ for the ξ axis (selecting the smallest γ) from

$$\frac{j \cdot \bar{a} \times \bar{b}}{i \cdot \bar{a} \times \bar{b}} = \frac{\sin\gamma \cos\beta}{\cos\gamma \cos\beta} = \tan\gamma = \frac{I_{yz}(I_x - I_z) + I_{xz}I_{xy}}{I_{yz}I_{xy} + I_{xz}(I_y - I_z)} \quad (D)$$

We determine β from

$$\begin{aligned} \frac{k \cdot \bar{a} \times \bar{b}}{i \cdot \bar{a} \times \bar{b}} &= \frac{-\sin\beta}{\cos\gamma \cos\beta} = -\frac{1}{\cos\gamma} \tan\beta \\ &= \frac{(I_x - I_z)(I_y - I_z) - I_{xy}^2}{I_{xy}I_{yz} + I_{xz}(I_y - I_z)} \end{aligned} \quad (E)$$

To determine α we rewrite equations (2) using $\lambda_2 = I_\eta$,

$$\begin{aligned} (I_x - I_\eta)p - I_{xy}q - I_{xz}r &= 0 = \bar{c} \cdot \bar{\Omega} \\ -I_{xy}p + (I_y - I_\eta)q - I_{yz}r &= 0 = \bar{d} \cdot \bar{\Omega} \end{aligned}$$

and we use the relationship

$$\frac{j \bar{c} \times \bar{d}}{k \bar{c} \times \bar{d}} = \sin \gamma \tan \beta + \frac{\cos \gamma}{\cos \beta} \tan \alpha \quad (F)$$

Because β, γ are small,

$$\frac{j \bar{c} \times \bar{d}}{k \bar{c} \times \bar{d}} \approx \tan \alpha$$

REFERENCES

1. Grantham, W. D., Effects of Mass-Loading Variations and Applied Moments on Motion and Control of a Manned Rotating Space Vehicle, NASA TN D-803 (1961).
2. Kurzahls, P. R. and C. R. Keckler, Spin Dynamics of Manned Space Stations, NASA TR R-155 (1963).
3. Adams, J. J., Study of an Active Control System for a Spinning Body, NASA TN D-905 (1961).

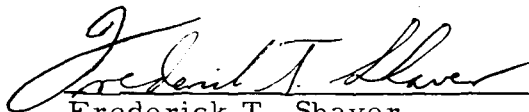
APPROVAL

DYNAMICS OF A ROTATING
SPACE STATION

By

Dr. Walter P. Krause

The information in this report has been reviewed for security classification. Review of any information concerning Department of Defense or Atomic Energy Commission programs has been made by the MSFC Security Classification Officer. This report, in its entirety, has been determined to be unclassified.


Frederick T. Shaver
Chief, Simulation Branch


H. Hoelzer
Director, Computation Laboratory

DISTRIBUTION

DIR

Dr. Wernher von Braun

DEP-T

Dr. Eberhard Rees

AST-S

Dr. O. H. Lange

R-DIR

Mr. H. K. Weidner

Dr. J. C. McCall

R-FP

Dr. H. H. Koelle

Dr. H. O. Ruppe

Mr. J. W. Carter

Mr. L. T. Spears

R-AERO

Dr. E. D. Geissler

Dr. R. F. Hoelker

Dr. F. A. Speer

Mr. H. J. Horn

Mr. P. J. DeFries

Mr. V. S. Verderaime

Mr. M. H. Rheinfurth

Mr. R. S. Ryan

Mr. D. Teuber

R-AERO-G

R-AERO-GA

R-AERO-D

R-AERO-DD

R-ASTR

Dr. W. Haeussermann

Dr. R. Decher

Mr. F. E. Digesu

Mr. W. Thornton

Mr. J. Pavlick

Mr. H. H. Hosenthien

Mr. J. Lucas

R-ASTR-N

R-ASTR-F

R-COMP

Dr. H. Hoelzer

Mr. C. L. Bradshaw

Mr. C. Prince

Mr. C. P. Hubbard

Dr. E. Fehlberg

Dr. R. F. Arenstorff

Mr. M. C. Davidson

Dr. H. Krenn

Dr. J. Morelock

Mr. F. T. Shaver (10)

Dr. W. P. Krause (10)

Mr. J. S. Spear

Mr. H. W. Zeanah

Mr. J. C. McCoy

Mr. G. E. Prince

Mr. F. L. Vinz

Mr. J. T. Howell

Mr. M. H. Knighton

R-ME

Mr. W. R. Kuers

Mr. H. Wuenscher

DISTRIBUTION
(Continued)

R-RP

Dr. E. Stuhlinger
Mr. G. B. Heller

R-P&VE

Dr. W. A. Mrazek
Mr. E. E. Goerner
Mr. C. R. Ellsworth (20)
Dr. H. G. Krause
Mr. M. Cash
Mr. L. R. Cohen

R-TEST

Mr. K. L. Heimburg
Dr. G. H. Reisig

M-MS-IP

General Electric Co.

Mr. H. R. Wrage
Mr. J. Albert
Dr. C. R. Cassity
Dr. J. F. Andrus
Mr. A. L. McGarrity
Mr. R. S. Johnson

AMICOM DR&D

Mr. O. H. Hirschler
Mr. E. F. Euterneck
Dr. H. B. Holl

Langley Research Center (3)

Manned Spacecraft Center (3)

NASA Headquarters

Mr. R. W. Taylor